Fast Computation of the Fundamental Matrix for an Active Stereo Vision System

Fuxing Li, Michael Brady, Charles Wiles

Department of Engineering Science, University of Oxford, Oxford OX1 3PJ

Abstract. This paper investigates the problem of computing the fundamental matrix for a class of active stereo vision system, namely with common elevation platform. The fundamental matrix is derived for such a system, and a number of methods are proposed to simplify its computation. Experimental results validate the feasibility of the different methods. These methods are then used in a real application to validate the correctness of the fundamental matrix form for an active stereo system. We demonstrate that typical variations in camera intrinsic parameters do not much affect the epipolar geometry in the image. This motivates us to calibrate the camera intrinsic parameters approximately and then to use the calibration results to compute the epipolar geometry directly in real time.

1 Introduction

Active stereo vision systems based on a common elevation platform have been widely used for research on the visual control and navigation of mobile robots [1]. Usually, this kind of vision system has four degrees of freedom. The two cameras have independent vergence joints and use a common elevation platform. A pan joint is used to increase the field of view of the system. There is a platform for each of the cameras so that their optical centres can be adjusted to a position near the intersection of the elevation axis and the vergence axes to ensure that the elevation and vergence of the head approximately causes a pure rotation of the cameras. Let P be the fixation point of the two cameras, θ_e the elevation angle of the system, and θ_l and θ_r the two camera angles. Clearly, the epipolar geometry depends only on the two vergence joint angles. When the cameras verge, the epipolar geometry changes dynamically.

Such a stereo head has been mounted on the mobile robot at Oxford University to provide visual information for navigation. With the LICA(*Locally Intelligent Control Agent*)[3] based distributed architecture, parallel implementation of a number of algorithms using on-board transputers makes real-time visual guidance practical. Using such a robot head, the vision system is able to actively change its geometry to adapt to the task requirements and to plan and execute accurate camera motions. We have demonstrated real-time target tracking and following using this method[1].

In order to solve the feature-based correspondence problem in real time, a fast method must be employed to compute the epipolar geometry, hence to limit

the search from two dimensions to one for correspondence. Furthermore, during the active verging process, all camera-related parameters are unchanged apart from the camera verge angles, which are available from the head state feedback.

In this paper, we investigate specific forms of the fundamental matrix, the algebraic representation of the epipolar geometry, for this important kind of stereo system. As a result, a number of methods are proposed to compute the fundamental matrix quickly and reliably. From extensive experimental results of applying these methods, epipolar geometry related camera intrinsic parameters are calibrated approximately. We demonstrate with these calibration results and the head state feedback, it is possible to update the epipolar geometry directly with sufficient accuracy. This will be applied to revisit the parallel implementation of PMF[5] in the near future and the result used to actively control the head.

2 The Common Elevation Fundamental Matrix

A stereo head with common elevation platform can be regarded as two cameras related by a translation $\mathbf{T}$ along the baseline and a rotation $\mathbf{R}$ about the Y axis. The fundamental matrix[8] is:

$$\mathbf{F} = \mathbf{C}'^{-\mathsf{T}}\mathbf{R}[\mathbf{T}]_{\mathbf{X}}\mathbf{C}^{-1} = \mathbf{C}'^{-\mathsf{T}}\mathbf{R}\mathbf{C}^{\mathsf{T}}[\mathbf{C}\mathbf{T}]_{\mathbf{X}},$$

where

$$\mathbf{C} = \begin{bmatrix} fk_u & 0 & u_0 \\ 0 & -fk_v & v_0 \\ 0 & 0 & 1 \end{bmatrix}, \quad \mathbf{T} = \begin{bmatrix} -Bsin\theta_l \\ 0 \\ -Bcos\theta_l \end{bmatrix}, \quad \mathbf{R} = \begin{bmatrix} cos\theta_v & 0 & sin\theta_v \\ 0 & 1 & 0 \\ -sin\theta_v & 0 & cos\theta_v \end{bmatrix},$$

The matrix $\mathbf{C}'$ is similar to $\mathbf{C}$. $\mathbf{C}$ and $\mathbf{C}'$ are the *camera calibration matrices* for the left and right cameras respectively, and represent the transformation from camera coordinates to image coordinates. B is the length of the stereo baseline; θ_l, θ_r are the left and right camera angles respectively; and $\theta_v = \theta_r - \theta_l$ is called the camera vergence angle.

We find that in this case $\mathbf{F}$ can be written in the following form:

$$\mathbf{F} = \begin{bmatrix} 0 & a & ab \\ c & 0 & d \\ b'c & e & b'd + be \end{bmatrix}, \tag{1}$$

where

$$a = \frac{fk_u}{fk'_u}cos\theta_r, \quad b = -v_0, \quad b' = -v'_0, \quad c = -\frac{fk_v}{fk'_v}cos\theta_l,$$
$$d = \frac{fk_v}{fk'_v}(fk_u sin\theta_l + u_0 cos\theta_l), \quad e = -(fk_u sin\theta_r + \frac{fk_u}{fk'_u}u'_0 cos\theta_r).$$

We will call this the common elevation fundamental matrix in the remainder of the paper.

The epipoles $\mathbf{e} = (e_x, e_y)^\top$ in the left image and $\mathbf{e}' = (e'_x, e'_y)^\top$ in the right image are:

$$e_x = -\frac{d}{c} = fk_u tan\theta_l + u_0, \quad e_y = -b = v_0,$$
$$e'_x = -\frac{e}{a} = fk'_u tan\theta_r + u'_0, \quad e'_y = -b' = v'_0.$$

Of the entries of the common elevation fundamental matrix:

$$d = \frac{fk_v}{fk'_v} sqrt(fk_u^2 + u_0^2) cos(\theta_l - \phi),$$

where $tan\phi = fk_u/u_0$.

For d to be zero, $cos(\theta_l - \phi) = 0$. This implies $\theta_l = \phi + \frac{2n+1}{2}\pi$; but $\phi \neq 0$ and $0° < \theta_l \leq 90^0$, so d is highly unlikely to be zero.

Since the fundamental matrix is only significant up to scale, using the property that d is unlikely to be zero, we set $d = 1$ in the following to simplify computations.

3 Computation

From equation 1, it can be seen that the main difference between the general fundamental matrix and that for a stereo head is that the latter has two zero entries which reflect the constraint of common elevation. That means we can compute the other entries with a simplified algorithm that is better conditioned and that can easily operate in real time.

8-point algorithm: Generally, each correspondence point pair generates one constraint on the fundamental matrix $\mathbf{F}$:

$$[x'_i\ y'_i\ 1] \begin{bmatrix} f_1 & f_2 & f_3 \\ f_4 & f_5 & f_6 \\ f_7 & f_8 & f_9 \end{bmatrix} \begin{bmatrix} x_i \\ y_i \\ 1 \end{bmatrix} = 0.$$

This can be rearranged as $\mathbf{Mf} = 0$ where $\mathbf{M}$ is a $n \times 9$ measurement matrix, and $\mathbf{f}$ is the fundamental matrix represented as a 9-vector:

$$\begin{bmatrix} x'_1x_1 & x'_1y_1 & x'_1 & y'_1x_1 & y'_1y_1 & y'_1 & x_1 & y_1 & 1 \\ \vdots & \vdots & \vdots & \vdots & \vdots & \vdots & \vdots & \vdots & \\ x'_nx_n & x'_ny_n & x'_n & y'_nx_n & y'_ny_n & y'_n & x_n & y_n & 1 \end{bmatrix} \begin{bmatrix} f_1 \\ \vdots \\ f_9 \end{bmatrix} = 0.$$

If the correspondence point pairs are reliable, 7 pairs suffice to solve $\mathbf{F}$ up to scale. To solve the problem linearly, it is customary to use 8 points to estimate f_i, $i = 1, \cdots, 9$, first and then enforce the zero determinant constraint afterwards[2].

6-point algorithm (linear method): After reparameterising the common elevation fundamental matrix from equation 1, we get

$$[x'_i\ y'_i\ 1] \begin{bmatrix} 0 & f_2 & f_3 \\ f_4 & 0 & 1 \\ f_7 & f_8 & f_9 \end{bmatrix} \begin{bmatrix} x_i \\ y_i \\ 1 \end{bmatrix} = 0.$$

This can be rewritten and solved using Singular Value Decomposition(SVD):

$$\begin{bmatrix} x'_1y_1 & x'_1 & y'_1x_1 & x_1 & y_1 & 1 \\ \vdots & \vdots & \vdots & \vdots & \vdots & \vdots \\ x'_ny_n & x'_n & y'_nx_n & x_n & y_n & 1 \end{bmatrix} \begin{bmatrix} f_2 \\ f_3 \\ f_4 \\ f_7 \\ f_8 \\ f_9 \end{bmatrix} = \begin{bmatrix} -y'_1 \\ \vdots \\ -y'_n \end{bmatrix}. \tag{2}$$

However, this does not ensure $det\mathbf{F} = 0$, and we have to enforce this constraint subsequently.

A convenient way to do this is to correct the matrix $\mathbf{F}$ found by equation 2. $\mathbf{F}$ is replaced by the matrix $\mathbf{F}'$ that minimises the Frobenius norm $||\mathbf{F}-\mathbf{F}'||$ subject to the condition $det\mathbf{F}' = 0$. This method was suggested by Tsai and Huang [7], adopted by Hartley [2], and has been proven to minimise the Frobenius norm $||\mathbf{F} - \mathbf{F}'||$, as required. Please consult [4] for details.

This kind of linear algorithm is normally not stable and is sensitive to noisy data. As Hartley argued in [2], normalising the data improves the performance of the eight point algorithm, which is used to compute the general form fundamental matrix. Our experimental results support this argument.

5-point algorithm (nonlinear method): Equation 1 can be written as:

$$\mathbf{F} = \begin{bmatrix} 0 & a & ab \\ c & 0 & 1 \\ b'c & e & b'+be \end{bmatrix} = \begin{bmatrix} 1 & 0 & 0 \\ 0 & 1 & 0 \\ 0 & b' & 1 \end{bmatrix} \begin{bmatrix} 0 & a & 0 \\ c & 0 & 1 \\ 0 & e & 0 \end{bmatrix} \begin{bmatrix} 1 & 0 & 0 \\ 0 & 1 & b \\ 0 & 0 & 1 \end{bmatrix}.$$

Let

$$\mathbf{F}' = \begin{bmatrix} 0 & a & 0 \\ c & 0 & 1 \\ 0 & e & 0 \end{bmatrix}, \quad \mathbf{T}' = \begin{bmatrix} 1 & 0 & 0 \\ 0 & 1 & b' \\ 0 & 0 & 1 \end{bmatrix}, \quad \mathbf{T} = \begin{bmatrix} 1 & 0 & 0 \\ 0 & 1 & b \\ 0 & 0 & 1 \end{bmatrix},$$

then

$$\mathbf{x}'^{\top}\mathbf{F}\mathbf{x} = \mathbf{x}'^{\top}\mathbf{T}'^{\top}\mathbf{F}'\mathbf{T}\mathbf{x} = (\mathbf{T}'\mathbf{x}')^{\top}\mathbf{F}'\mathbf{T}\mathbf{x} = 0,$$

ie.

$$[x'_i \; y'_i + b' \; 1] \begin{bmatrix} 0 & a & 0 \\ c & 0 & 1 \\ 0 & e & 0 \end{bmatrix} \begin{bmatrix} x_i \\ y_i + b \\ 1 \end{bmatrix} = 0.$$

Now we have five free parameters. In theory, given five correspondence point pairs, we should be able to solve for them. However this is a nonlinear problem.

If b and b' are unknown, the problem can be formed as a nonlinear optimisation problem to find b and b' to minimise

$$\sum (x'_i(y_i + b)a + x_i(y'_i + b')c + (y_i + b)e + (y'_i + b'))^2,$$

where a, c, e are computed to produce the sum of squares using SVD, given a set of b and b', as follows:

$$x'_i(y_i + b)a + x_i(y'_i + b')c + (y_i + b)e = -(y'_i + b').$$

3-point algorithm A (linear method with known b and b'): If the cameras are partially calibrated, ie. b and b' are known, then from the previous section, we can omit the nonlinear process and use SVD to solve a, c, e directly as follows:

$$[x_i'(y_i+b)\ x_i(y_i'+b')\ (y_i+b)]\begin{bmatrix}a\\c\\e\end{bmatrix} = -(y_i'+b')$$

4-point algorithm: If (as is often reasonable in practice) we assume that the two cameras forming the stereo head have approximately the same intrinsic parameters, the fundamental matrix can be further simplified:

$$\mathbf{F} = \begin{bmatrix} 0 & cos\theta_r & -v_0 cos\theta_r \\ -cos\theta_l & 0 & fk_u sin\theta_l + u_0 cos\theta_l \\ v_0 cos\theta_l & -(fk_u sin\theta_r + u_0 cos\theta_r) & u_0 v_0(cos\theta_r - cos\theta_l) + fk_u v_0(sin\theta_r - sin\theta_l) \end{bmatrix}$$
$$= \begin{bmatrix} 0 & a & ab \\ c & 0 & d \\ bc & e & b(d+e) \end{bmatrix},$$

where

$$a = cos\theta_r, \quad b = -v_0, \quad c = -cos\theta_l,$$
$$d = fk_u sin\theta_l + u_0 cos\theta_l, \quad e = -fk_u sin\theta_r - u_0 cos\theta_r.$$

As before, we can set $d = 1$.

If we further set $r = \frac{a}{c}$, the fundamental matrix becomes:

$$\mathbf{F} = \begin{bmatrix} 0 & rc & rcb \\ c & 0 & 1 \\ bc & e & b(1+e) \end{bmatrix}. \tag{3}$$

There are four free parameters b, c, e and r. In theory, with four correspondence point pairs, we should be able to solve for them. This is also a nonlinear problem. Compared to the situation when the two cameras have different intrinsic parameters, the nonlinearity is caused by just one parameter b. We can derive the nonlinear equation of b given four correspondence point pairs, then a regression method can be used to solve for b. Please consult [4] for details.

3-point algorithm B (camera angles are known): For an active vision system, we can usually acquire the head state, hence the camera angles θ_l and θ_r. In this case, $r = \frac{a}{c} = \frac{cos(\theta_r)}{-cos(\theta_l)}$ is known since it relies only on the camera angles whatever scale the fundamental matrix uses. We can then further simplify the 4-point algorithm to be the 3-point algorithm B.

Given three correspondence point pairs, we can derive a quadratic equation for b from the definition of the fundamental matrix. It is very easy to determine its closed form solution and then compute parameters c, e and a. Please consult [4] for details.

From the formula for the fundamental matrix, we can see that although we set $d = 1$, which scales the parameters which form the fundamental matrix, this

does not affect the value of b, so b remains equal to $-v_o$. We can guess its initial value, and this can be used to select one of the two solutions of the quadratic.

Random sampling [6] is used to choose the best three point pairs to compute the fundamental matrix with the above algorithm. Another benefit of using the 4-point algorithm and 3-point algorithm B discussed in this section is they can be used to distinguish inliers and outliers of correspondence pairs.

4 Results

We have performed extensive experiments on synthetic and real data, [4] gives details. We present results here for a typical experiment on real data.

An image pair of a calibration grid standing in our laboratory was taken from our active stereo head with camera angles $\theta_l = 75^o$ and $\theta_r = 105^o$. The camera vergence angle is 30^o which is usually the maximum value in real applications.

The number of the inliers among the point pairs used in the computation is one of the criteria to evaluate the quality of the computed fundamental matrix. If $d_i = \frac{d(p_i', Fp_i) + d(p_i, F^\top p_i')}{2} < d_t$, we say that the computed fundamental matrix fits for the point pair (p_i, p_i'), and point pair (p_i, p_i') is a inlier. Here $(p_i, p_i'), i = 1, \cdots, n$, are the n correspondence point pairs and $d(\cdot, \cdot)$ is the point-to-line Euclidean distance expressed in pixels. d_t is the threshold value which reflects the quality of the computed fundamental matrix as another criterion.

The fundamental matrices computed by the different algorithms are listed in Table 1, and we give the numbers of inliers in the table explicitly, given $d_t < 1$. We do not compute results using the 3-point A algorithm, since we do not know the true values of b and b'.

The results show that the first two diagonal elements are indeed close to zero when the 8-point and 6-point algorithms are used. The small difference from zero in these elements may be due to small manufacturing errors and slight misalignment in the common elevation geometry. However, we observe that the epipolar geometry computed by the 8-point and 6-point algorithms (see Figure 1) is in fact consistent with the plane to plane homography of the grid in the foreground of the scene. We conclude that, in this example, the point set used to compute the epipolar geometry must be close to approximating a plane and hence the computation of epipolar geometry with the 8-point and 6-point algorithms is underconstrained, resulting in a number of equally valid geometries close to that computed above. The 5-point algorithm enforces the leading diagonal elements to equal zero and hence limits the epipolar geometry to a unique solution. In fact the epipolar geometry computed with the 5-point algorithm more acurately approximates the true epipolar geometry of the stereo rig.

The results for the 4-point and 3-point B algorithms are poor, suggesting that the assumption of identical intrinsic parameters is not valid in this case (thus we do not show their epipolar lines in Figure 1).

Note that although the epipoles computed by the different algorithms are quite different, the large variation in b and b' does not significantly affect the

Table 1. *The results of the epipolar geometry computed by different algorithms for a stereo image pair. The first column is the algorithm used, the second the computed F matrix, the third the epipoles, and the fourth the number of inliers and total number of points considered. The corresponding epipolar lines are shown in Figure 1.*

8-pt	$\mathbf{F} = \begin{bmatrix} 0.000049 & -0.000707 & 0.058852 \\ -0.000720 & -0.000045 & 1.000000 \\ 0.122604 & -0.809891 & -23.999954 \end{bmatrix}$	$\mathbf{e} = \begin{bmatrix} 1389.71 \\ 83.2074 \end{bmatrix}, \mathbf{e}' = \begin{bmatrix} -1145.06 \\ 170.384 \end{bmatrix}$	20/20
6-pt	$\mathbf{F} = \begin{bmatrix} -0.000043 & -0.000241 & 0.063241 \\ -0.001126 & -0.000000 & 1.000000 \\ 0.129292 & -0.879739 & -23.914293 \end{bmatrix}$	$\mathbf{e} = \begin{bmatrix} 888.455 \\ 262.196 \end{bmatrix}, \mathbf{e}' = \begin{bmatrix} -3647.36 \\ 114.87 \end{bmatrix}$	20/20
5-pt	$\mathbf{F} = \begin{bmatrix} 0 & -0.000620 & 0.080674 \\ -0.000804 & 0 & 1 \\ 0.108096 & -0.830662 & -26.2668 \end{bmatrix}$	$\mathbf{e} = \begin{bmatrix} 1242.7 \\ 130.094 \end{bmatrix}, \mathbf{e}' = \begin{bmatrix} -1339.51 \\ 134.331 \end{bmatrix}$	20/20
4-pt	$\mathbf{F} = \begin{bmatrix} 0 & -0.002125 & 0.918267 \\ 0.002209 & 0 & 1 \\ -0.954708 & -0.717975 & -121.866 \end{bmatrix}$	$\mathbf{e} = \begin{bmatrix} -452.60952 \\ 432.109 \end{bmatrix}, \mathbf{e}' = \begin{bmatrix} -337.85787 \\ 432.109 \end{bmatrix}$	12/20
3-pt B	$\mathbf{F} = \begin{bmatrix} 0 & -0.000766 & 0.128619 \\ -0.000766 & 0 & 1 \\ 0.128619 & -0.786932 & -35.7733 \end{bmatrix}$	$\mathbf{e} = \begin{bmatrix} 1305.3757 \\ 167.896 \end{bmatrix}, \mathbf{e}' = \begin{bmatrix} -1027.2419 \\ 167.896 \end{bmatrix}$	9/20

epipolar lines in the image (since they are far from the image center). We discuss this further in section 5.

The analysis presented above assumes that the common elevation stereo head has been manufactured perfectly; but in practice this is never the case. The upshot of this is that intrinsic parameters that should be identical are measured to be different, and even though manufacturing errors may be slight the corresponding errors in the intrinsic parameters can be huge. In related work [4], we have shown how the fundamental matrix can be used to identify (small) manufacturing errors and correct for them in software automatically. Here, for purposes of clarity in exposition, we assume that slight manufacturing errors have been identified and corrected for. Please consult [4] for details.

5 Calibration

Our experiments show that the variation of b and b' does not much affect the epipolar lines in the image. If this is true for all the intrinsic parameters, we can then calibrate them using algorithms for computing the common elevation fundamental matrix and use the calibration results to compute the fundamental matrix directly according to its theoretical form.

We have studied the effects of intrinsic parameter variation on the epipolar geometry. Table 2 shows a typical result, corresponding to variations in the estimation of u_0. Here $(e_x, e_y)^\top$ is the epipole in the left image, $(e'_x, e'_y)^\top$ is the epipole in the right image, d_{cl} represents the corner-to-epipolar line distance in

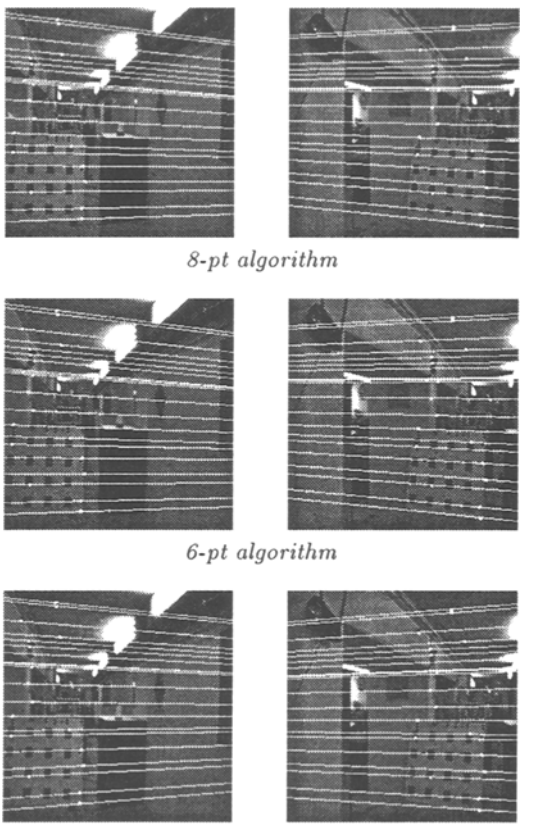

Fig. 1. *Epipolar lines computed by various algorithms for an image pair. The corresponding fundamental matrices are shown in Table 1.*

the left image, d'_{cl} represents the corner-to-epipolar line distance in the right image, s represents the slope of the epipolar line in the left image, s' represents the slope of the epipolar line in the right image, E and σ represents the mean value and the standard deviation of the correspondence variable on the table. 500 randomly selected stereo match pairs are used for the statistical computation.

Table 2. *The error mean and covariance about epipolar geometry when u_o changes.*

Variation	10%				30%			
Vergence	10^o		30^o		10^o		30^o	
	E	σ^2	E	σ^2	E	σ^2	E	σ^2
e_x	12	0	12	0	36	0	36	0
e_y	0	0	0	0	0	0	0	0
e'_x	12	0	12	0	36	0	36	0
e'_y	0	0	0	0	0	0	0	0
d_{cl}	0.46104	0.119537	1.01775	0.504995	1.03841	0.542331	2.83341	3.64044
d'_{cl}	0.460199	0.11874	1.02727	0.510776	1.04803	0.546761	2.96384	3.94416
s	0.229193	1.11552	0.479116	8.44234	0.747675	1.98968	1.37208	11.4518
s'	-0.0305518	0.788074	-0.313323	6.92041	0.0892043	0.917001	-0.655556	7.11436

It is clear that when the vergence angle is less than 30^o, the epipoles are far from the image planes, so that the epipolar lines change very little when the camera intrinsic parameters change slightly. In particular, the corner-to-epipolar line distance, which is used to measure the accuracy of the epipolar geometry, changes very little. This enables us to approximate calibration to compute the epipolar geometry efficiently.

We are able to get the nearly constant b and b', which represent the image centre's vertical coordinate in each image, for the left and right images of different frames using the algorithms for computing the common elevation fundamental matrix proposed in this paper. If we can obtain the other camera intrinsic parameters based on which the epipolar geometry can be computed, we can update the epipolar geometry using the stereo head state feedback in real time.

If we assume that the remaining intrinsic parameters are indeed equal between the two cameras such that $fk_u = fk'_u$ and $u_0 = u'_0$, then we can compute them given the camera angles θ_l and θ_r. The theoretical form of the common elevation fundamental matrix when the two cameras have the same value between fk_u and fk'_u, u_0 and u'_0 but different value between v_0 and v'_0 is:

$$\mathbf{F} = \begin{bmatrix} 0 & cos\theta_r & -v_0 cos\theta_r \\ -cos\theta_l & 0 & fk_u sin\theta_l + u_0 cos\theta_l \\ v'_0 cos\theta_l & -(fk_u sin\theta_r + u_0 cos\theta_r) & v_0(fk_u sin\theta_r + u_0 cos\theta_r) - v'_0(fk_u sin\theta_l + u_0 cos\theta_l) \end{bmatrix}. \quad (4)$$

Given the camera angles and v_0, v'_0 approximately, we can use SVD to compute fk_u and u_0 according to known stereo match pairs:

$$[sin(\theta_l)(y' - v'_0) - sin(\theta_r)(y - v_0)\ cos(\theta_l)(y' - v'_0) - cos(\theta_r)(y - v0)] \begin{bmatrix} fk_u \\ u_0 \end{bmatrix}$$
$$= (\mathrm{y}' - \mathrm{v}'_0)\mathrm{x} * \cos(\theta_\mathrm{l}) - (\mathrm{y} - \mathrm{v}_0)\mathrm{x}'\cos(\theta_\mathrm{r}).$$

The more the camera verges, the more accurate the intrinsic parameters we can compute from the fundamental matrix according to the stereo match pairs. We use stereo match pairs from the image pair with vergence angle 30^o.

The calibration results are then used to compute the fundamental matrix according to equation 4 for real image pairs taken from our active stereo head with different vergence angles. The computed fundamental matrices are sufficiently accurate for stereo correspondence search. [4] gives details of these results. This means that using this approximate calibration results, we can then compute the fundamental matrix in real time with the head state feedback. The calibration algorithm is listed in Figure 2, and a typical result is shown in Table 3.

References

1. F. Du and J.M. Brady. A four degree-of-freedom robot head for active vision. *International Journal of Pattern Recognition and Artificial Intelligence*, 8(6) 1994.
2. R. Hartley. In defence of the 8-point algorithm. In *Procceding of ICCV'95 International Conference on Computer Vision*, pages 1064–1070, 1995.
3. H. Hu, M. Brady, J. Grothusen, F. Li, and P. Probert. Licas: A modular architecture for intelligent control of mobile robots. In *Procceding of IROS'95 International Conference on Intelligent Robots and Systems*, 1995.

Input $I_l(0), I_r(0)$: Image pair with parallel geometry;
$I_l(30), I_r(30)$: Image pair verged 30^o;
Output fk_u, u_0, v_0, v_0' : Camera intrinsic parameters.

1. Obtain the stereo match pairs for each image pair using the 8-point algorithm.

$$\mathbf{F} = \begin{bmatrix} f_1 & f_2 & f_3 \\ f_4 & f_5 & f_6 \\ f_7 & f_8 & f_9 \end{bmatrix};$$

2. Identify and correct small manufacturing errors[4] so that both fundamental matrices have the form:

$$\mathbf{F} = \begin{bmatrix} 0 & a & ab \\ c & 0 & 1 \\ b'c & e & b' + be \end{bmatrix},$$

where $b' = b + \delta b$. δb is obtained in this step by identify small manufacturing errors[4];

3. Compute $v_0 = -b$ and $v_0' = -b' = -(b + \delta b)$ using the 5-point algorithm from:

$$\mathbf{F(30)} = \begin{bmatrix} 0 & a & ab \\ c & 0 & 1 \\ b'c & e & b' + be \end{bmatrix};$$

4. Compute fk_u and u_0 using SVD from:

$$\begin{bmatrix} sin(\theta_l)(y' - v_0') - sin(\theta_r)(y - v_0) & cos(\theta_l)(y' - v_0') - cos(\theta_r)(y - v0) \end{bmatrix} \begin{bmatrix} fk_u \\ u_0 \end{bmatrix} = (y' - v_0')x * cos(\theta_l) - (y - v_0)x' cos(\theta_r),$$

here $\theta_l = 75^o$, $\theta_r = 105^o$. v_0 and v_0' are computed from the above step.

Fig. 2. *The algorithm of calibrating the camera intrinsic parameters for computing the epipolar geometry.*

Table 3. *The results of the epipolar geometry for different image pairs using the calibration parameters and camera angles. The first column is the vergence angle, the second the computed F matrix, the third the epipoles, and the fourth the number of inliers and total number of points considered.*

Parallel image pair	$\mathbf{F} = \begin{bmatrix} -0.000000 & -0.000000 & 0.024713 \\ -0.000000 & 0.000000 & 1.000000 \\ 0.001243 & -1.000000 & -4.720147 \end{bmatrix}$	$\mathbf{e} = \begin{bmatrix} 8.2e+07 \\ 7.1e+07 \end{bmatrix}$, $\mathbf{e}' = \begin{bmatrix} -2.9e+09 \\ 102441 \end{bmatrix}$	19/20
20^o	$\mathbf{F} = \begin{bmatrix} -0.000011 & -0.000479 & 0.078777 \\ -0.000479 & 0.000011 & 1.000000 \\ 0.058886 & -0.879146 & -21.207220 \end{bmatrix}$	$\mathbf{e} = \begin{bmatrix} 2088.92 \\ 164.534 \end{bmatrix}$, $\mathbf{e}' = \begin{bmatrix} -1836.19 \\ 123.009 \end{bmatrix}$	20/20

4. F. Li, J.M. Brady, and C. Wiles. Calibrating the camera intrinsic parameters for epipolar geometry computation. Technical report, OUEL 2075/1995, 1995.
5. Stephen B Pollard, John Porrill, John E W Mayhew, and John P Frisby. Disparity gradient, lipschitz continuity, and computing binouclar correspondences. In John E W Mayhew and John P Frisby, editors, *3D Model Recognition From Stereoscopic Cues*, pages 25–32. MIT, 1991.
6. P. Torr. *Motion Segmentation and Outlier Detection.* PhD thesis, University of Oxford, 1995.
7. R. Y. Tsai and T. S. Huang. Uniqueness and estimation of three dimensional motion parameters of rigid objects with curved surfaces. *IEEE Trans. Patt. Anal. Machine Intell.*, PAMI-6:13–27, 1984.
8. A. Zisserman. The geometry of multiple views. Seminar note for computer vision, 1995.